Arch Pharm Res Vol 33, No 8, 1193-1198, 2010
DOI 10.1007/s12272-010-0809-x

Archives of Pharmacal Research
www.springer.com/12272

Preparation, Characterization, and *In Vivo* Evaluation of Mitoxantrone-loaded, Folate-conjugated Albumin Nanoparticles

Liang-ke Zhang[1,3], Shi-xiang Hou[2], Jing-qin Zhang[1], Wen-jing Hu[1], and Cheng-yuan Wang[4]

[1]Institute of Life Sciences, School of Pharmacy, Chongqing medical university, Chongqing 400016, China, [2]West China School of Pharmacy, Sichuan University, Chengdu 610041, China, [3]Chongqing Engineering Research Center of Medicine, Chongqing Medical University, Chongqing 400016, China, and [4]Research Center of Medical Chemistry & Chemical Biology, Chongqing Technology and Business University, Chongqing 400067, China

(Received November 4, 2009/Revised Frebuary 22, 2010/Accepted April 11, 2010)

Folic acid was covalently conjugated to bovine serum albumin nanoparticles (BSANP) to target the nanoparticles to SKOV3 cells expressing folate receptors. Mitoxantrone was incorporated into the folate-conjugated albumin nanoparticles, and the final nanoparticle size was 68 nm, as measured by a laser light scattering particle analyzer. The cytotoxic activity of mitoxantrone-loaded, folate-conjugated albumin nanoparticles (MTO-BSANP-folate), which was quantitated by ^{3}H-thymidine incorporation, was higher than mitoxantrone-loaded BSANP (MTO-BSANP) and MTO solution, and could be inhibited by free folic acid. MTO-BSANP-folate may be endocytosed via the folate receptor on the surface of SKOV3 cells. MTO-BSANP-folate also inhibited tumor growth better than the MTO-BSANP and MTO solution *in vivo*. These results indicate that folate-conjugated BSANP may have therapeutic potential as a vector for anticancer drugs in cancer chemotherapy.

Key words: Mitoxantrone, Folate-conjugated, Albumin nanoparticles

INTRODUCTION

Mitoxantrone (MTO) (Ehninger et al., 1990) is a cytotoxic anthracenedione derivative that intercalates with DNA and inhibits topoisomerase II. MTO is used for the treatment of breast cancer, ovarian carcinoma, acute leukemia, malignant lymphomas, and hepatocellular carcinoma (Smith, 1983; Shenkenberg and Von Hoff, 1986; Ehninger et al., 1990; Faulds et al., 1991; Schleyer et al., 1994). The dose-limiting toxicity of the anthracenedione derivative is myelosuppression combined with a weak cardiotoxicity (Faulds et al., 1991; Reszka et al., 1997). One way to avoid toxic side effects is to change pharmacological behavior with colloidal delivery systems. Many anticancer drugs have been incorporated in or associated with drug carrier systems such as liposomes or nanoparticles (Xiong et al., 2005; Lu et al., 2006; Dreis et al., 2007; Yang et al., 2007). In particular, protein-based colloidal systems show biodegradability, lack of toxicity and antigenicity, stability, a good shelf life, controllable drug-release properties, and high loading capacity for hydrophilic molecules (Rubino et al., 1993).

Colloidal carriers that incorporate cell-specific ligands can improve target efficiency. Folate receptors (FR) are overexpressed on the surface of cancer cells, but rarely found on normal cells, or they are localized to the apical surfaces of polarized epithelia (Lu and Low, 2003). Folate receptors are therefore tumor markers, especially in ovarian carcinomas (Campbell and Low, 1991). Folic acid, which binds folate receptors, is stable, inexpensive, and nonimmunogenic compared with other proteins such as monoclonal antibodies. Folic acid also binds to folate receptors with very high affinity (Kd = ~1 nM) and can be internalized by receptor-mediated endocytosis (Kamen and Caston, 1986; Lee and Low, 1994, 1995; Lee and Huang, 1996; Atkinson et al., 2001). Folate-conjugated liposomes can be internalized by receptor-bearing tumor cells via folate receptor-mediated endocytosis (Zhao and Lee, 2004; Chan et al., 2007). Other folate conjugates such

Correspondence to: Liang-ke Zhang, Institute of Life Sciences, School of Pharmacy, Chongqing medical university, Chongqing 400016, China
Tel: 86-23-6848-5078
E-mail: zlkdyx@gmail.com

as protein toxins, anti-T-cell receptor antibodies, radioimaging agents, chemotherapy agents, and gene transfer vectors also show receptor-specific delivery properties (Lu and Low, 2003).

We previously prepared folate-conjugated bovine serum albumin nanoparticles (BSANP) with folate conjugation levels of 169 μmol/g BSA. The uptake of folate-conjugated BSANP to SKOV3 cells was saturable and could be inhibited by folic acid, suggesting that internalization was mediated by the folate receptor (Zhang et al., 2004). Here, we incorporated mitoxantrone into the folate-conjugated BSANP and examined the cytotoxic effect and antitumor activity of MTO-BSANP-folate.

MATERIALS AND METHODS

Materials

A cryogenic ultracentrifuge (L8-50M, Beckmann) and magnetic stirrer (model 85-2, Sile Instrument Co.) were used for nanoparticle preparation. A laser particle sizer (Mastersizer 2000) and a transmission electron microscope (H-600, HITACHI Co.) were used to characterize the nanoparticles. A spectrophotometer (UV-2201, Shimazu) was used to determine the drug content in solution.

Folic acid, dicyclohexylcarbodiimide (DCC), and *N*-hydroxysuccinimide were all purchased from Sigma. Bovine serum albumin (BSA) was purchased from Boao Biotech Co. Ltd. MTO was supplied by Sichuan Shenghe Pharmaceutical Co. Ltd. ^{3}HTdR was obtained from Shanghai Institute of Nuclear Research Academia Sinica. SKOV3, a human ovarian cancer cell line, was a gift from the immunology laboratory of Sichuan University. RPMI-1640 medium without folic acid was obtained from Gibco. Female Balb/c mice, aged 6-8 weeks (20 ± 2 g), were purchased from the Sichuan Industrial Institute of Antibiotics. All other reagents were of analytical grade.

Preparation of folate-conjugated BSANP

Folate-conjugated BSANP was prepared by our method (Zhang et al., 2004). Briefly, BSA (10mg) was dissolved in 1 mL of purified water. Under constant stirring, desolvation of the 1% BSA solution was achieved by dropwise addition of 6 mL ethanol. After the desolvation process, 25 μL of 0.25% glutaraldehyde solution was added to induce particle crosslinking by stirring for 24 h (Weber et al., 2000; Langer et al., 2003). The suspension was centrifuged and the nanoparticles were redispersed in the original volume of water.

The *N*-hydroxysuccinimide ester of folic acid (NHS-folate) was prepared as described (Lee and Low, 1994). For conjugation, NHS-folate (50 mg) was dissolved in 1 mL of dimethyl sulfoxide and added slowly to the stirring BSANP suspension (2 mL, pH was adjusted to 10 using 1 M carbonate/bicarbonate buffer). After stirring for 45 min at room temperature, the reaction mixture was passed down a Sephadex G-50 column to separate the folate-conjugated BSANP from unreacted folic acid and other by-products. The folate-conjugated BSANP eluted in the void fraction.

Preparation of mitoxantrone-loaded, folate-conjugated BSANP

One milliliter of folate-conjugated BSANP suspension (containing 10 mg BSA) was centrifuged and the nanoparticles were redispersed to the original volume in carbonate/bicarbonate buffer (pH 9.0, 5 mM). Mitoxantrone (1.0 mg total as 100 μL of 10 mg/mL) was added to the dispersion and stirred for 30 min, then 50 μL of 0.25% glutaraldehyde was added to induce further crosslinking, and the suspension was centrifuged and redispersed with ultrasound.

Determination of the particle size

The size of albumin nanoparticles was determined by a Malvern Mastersizer-2000 laser light scattering particle analyzer (Malvern Instruments Ltd.). The samples were diluted with distilled water and measured at room temperature.

Transmission electron microscopy (TEM)

The size and morphology of nanoparticles were observed using a Hitachi H-600 Electron Microscope. A carbon-coated 200-mesh copper specimen grid was glow-discharged for 1.5 min. One drop of nanoparticle suspension was deposited on the grid and allowed to stand for 1.5 min. After removing excess fluid with filter paper, the grid was later stained with one drop of 2% phosphotungstic acid and allowed to dry in air for 10 min before examination under the electron microscope.

Evaluation of MTO encapsulation

The MTO-BSANP-folate or MTO-BSANP were washed three times with water by centrifugation at 20,000 × g for 20 min and digested with trypsin (0.05 mg/mg BSA). The digesting process was performed under stirring at 37°C for 2 h. After tryptic hydrolysis, encapsulation efficiency of the MTO-BSANP-folate was determined by a spectrophotometric analysis at an absorbance of 609 nm.

Measurement of Mitoxantrone release of mitoxantrone-loaded BSANPs *in vitro*

Ten milliliters of mitoxantrone-loaded BSANP suspension were added to a dialysis bag (cut-off molecular weight was 8000-12,000), and immersed into a flask containing 20 mL of phosphate buffer solution containing 0.1% (w/v) NaS_2O_5 (PBS 7.4, 0.1% NaS_2O_5). The sample flasks were incubated in a shaker bath at 50 rpm and 37°C. The release medium was sampled regularly and 5 mL of fresh PBS was replaced to continue the release test. The sampled release medium was measured by a UV-Vis spectrophotometer at 609 nm and compared to a mitoxantrone standard curve.

Cytotoxicity studies

SKOV3 cells in folate-depleted RPMI 1640 were seeded in 96-well plates at 10^3 cells/well (six replicates). 24 h later, cells were exposed for 2 h to MTO solution, MTO-BSANP, or MTO-BSANP-folate with or without 1 mmol/L free folic acid. The cells were washed twice and incubated further for 48 h in drug-free medium. 14 to 16 h before cells were harvested, 1 μCi/mL ^{3}H-thymidine was added to each well. Cells were then hydrolyzed with trypsin and collected. The count per minute (cpm) value was assayed after drying in air (Huang et al., 1999).

The survival rate of SKOV3 cells were calculated as:

$$\text{Survival rate (\%)} = B/A \times 100\%$$

where A is cpm of the control group, and B is that of the treatment group.

Animal model

The Sichuan University Animal Ethical Experimentation Committee, according to the requirements of the National Act on the Use of Experimental Animals, approved all procedures of the *in vivo* studies. Female Balb/c mice, aged 6-8 weeks (20 ± 2 g), were purchased from Sichuan Industrial Institute of Antibiotics.

SKOV3 cells (1×10^6) were subcutaneously transplanted into the mice. When tumor diameter reached approximately 7 mm, the mice were sacrificed and tumors were collected and cut into pieces of the same volume. The xenograft model was obtained by subcutaneously implanting tumor pieces into 20 female mice. Mice were fed a special low-folate diet (Sichuan Industrial Institute of Antibiotics) from 1 week before tumor inoculation until sacrifice.

In vivo chemotherapy studies

Experiments were performed on day 10 after tumor inoculation. Animals were randomly divided into five mice/group:

I. physiological saline
II. MTO solution (2.0 mg/kg body weight)
III. MTO-BSANP (2.0 mg/kg body weight)
IV. MTO-BSANP-folate (2.0 mg/kg body weight)

The treatments (all *i.v.* in the tail vein) were repeated every two days for three treatments. Tumor volume was measured over 20 days. Mice were sacrificed 9 days after post treatment and the tumor weight was measured. The tumor volumes and the inhibition rate of tumor growth (*IR*) were calculated as follows:

$$\text{Volume} = \pi \times L \times W^2/6$$

where L is the longest dimension parallel to the skin surface and W is the dimension perpendicular to L and the surface

$$IR\ (\%) = [(A - B)/A] \times 100\%$$

where A is average tumor weight of the control group, and B is that of the treatment group.

RESULTS AND DISCUSSION

Determination of particle size and transmission electron microscopy

The nanoparticles were spherical, with diameters less than 150 nm (Fig. 1). Laser light scattering measurements (Fig. 2) give a similar trend, with average diameters of MTO-BSANP-folate of 68 nm and MTO-BSANP of 65 nm, favoring the enhanced permeability and retention effect (EPR) as observed in most solid tumors (Singh and Lillard, 2009).

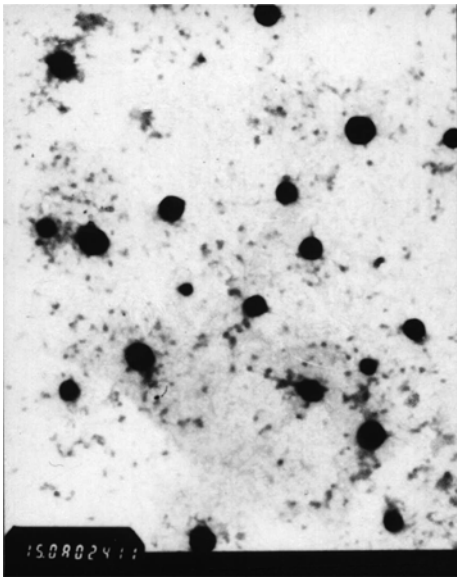

Fig. 1. TEM photo of MTO-BSANP-folate (× 15,000)

The encapsulation efficiency and *in vitro* release properties of MTO-BSANP-folate and MTO-BSANP

The maximum absorption wavelengths of MTO in enzymatic hydrolysate and release medium were 609 nm. For determination of encapsulation efficiency of MTO-BSANP-folate and MTO-BSANP, samples (supernatant after centrifugation) were diluted with PBS and measured spectrophotometrically after tryptic hydrolysis at 609 nm using equation (A): $A_{609\ nm} = 0.036C - 0.0083$, $r = 0.9997$ (4.05-24.39 μg/mL). For *in vitro* release tests, MTO samples were diluted with PBS, and determined spectrophotometrically at 609 nm using equation (B): $A_{609\ nm} = 0.033C - 0.017$, $r = 0.9998$ (4.02-24.12 μg/mL).

The encapsulation efficiency of MTO-BSANP-folate was 93.55% ± 0.89%, and that of MTO-BSANP was 93.81% ± 0.98%. Ascorbic acid (1.0% w/v) can improve stability of the MTO solution (Zhang and Liao, 1997). We added 0.1% (w/v) NaS_2O_5 to PBS (7.4) as an antioxidant, as this solution had a higher pH that was closer to physiological values, with suitable stability.

Fig. 3 shows the MTO release profiles of MTO-BSANP-folate and MTO-BSANP in PBS at 37°C. During the first 2 h, the initial MTO burst release from MTO-BSANP-folate and MTO-BSANP was less than 10%, with the remaining drug released gradually over the following 67 h, potentially enabling the maintenance of effective drug levels in the target organ. The drug release profiles were similar, with MTO-BSANP-folate fitting a bi-exponential equation: $1\text{-}Q = 0.437925e^{-0.00759t} + 0.714115e^{-0.16877t}$ ($r = 0.9945$), and that of MTO-BSANP fitting: $1\text{-}Q = 0.430012e^{-0.01416t} + 0.592621e^{-0.11214t}$ ($r = 0.9982$) (Fig. 3).

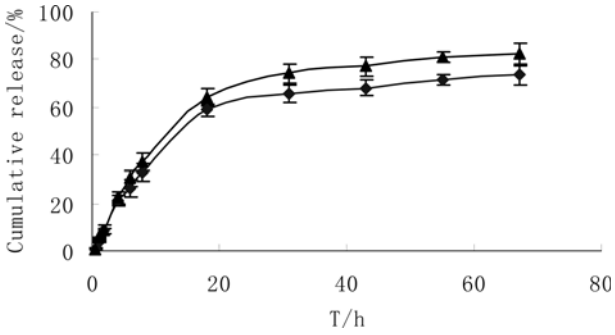

Fig. 3. *In vitro* release of MTO from MTO-BSANP-folate and MTO-BSANP in PBS (containing 0.1% (w/v) NaS_2O_5) at 37°C. ◆ - ◆, MTO-BSANP-folate; ▲ - ▲, MTO-BSANP

In vitro cytotoxic activity of MTO-BSANP-folate, MTO-BSANP, or MTO solution

SKOV3 cells were exposed to MTO solution, MTO-BSANP, MTO-BSANP-folate with or without 1 mmol/L free folic acid for 2 h, then washed and further incubated for 48 h in fresh medium. Only a small fraction of BSANP was internalized by SKOV3 cells for the first 2 h, as we showed previously (Zhang et al. 2004), so MTO-BSANP was the least cytotoxic. The cytotoxicity of MTO-BSANP-folate was higher than that of MTO-BSANP and MTO solution, and could be inhibited by the addition of free folic acid (Fig. 4), as we showed previously (Zhang et al. 2004), suggesting that MTO-BSANP-folate might be endocytosed via the folate receptor.

Therapeutic effects

Both MTO-nanoparticle preparations were more potent at inhibiting tumor growth than the MTO solution, putatively due to the EPR effects (Table I). The MTO-BSANP-folate group showed the most significant anti-

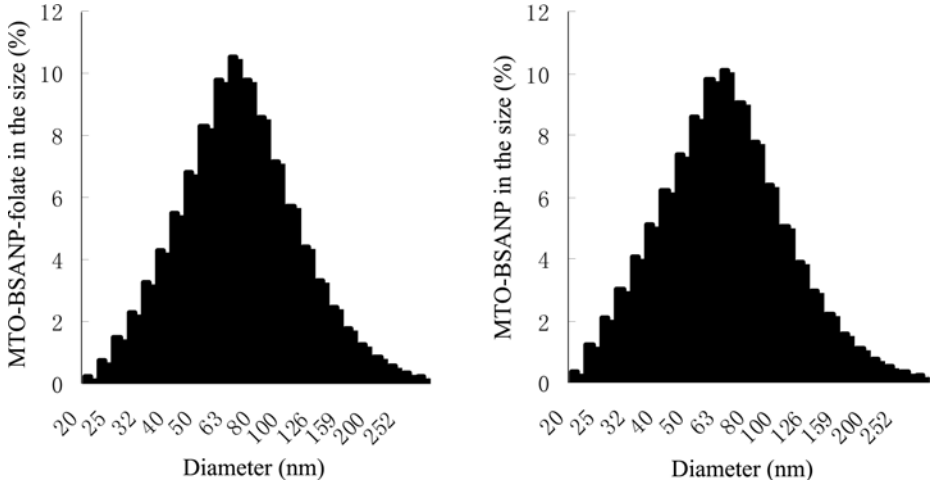

Fig. 2. Size distribution of MTO-BSANP-folate (left) and MTO-BSANP (right) as measured by laser light scattering

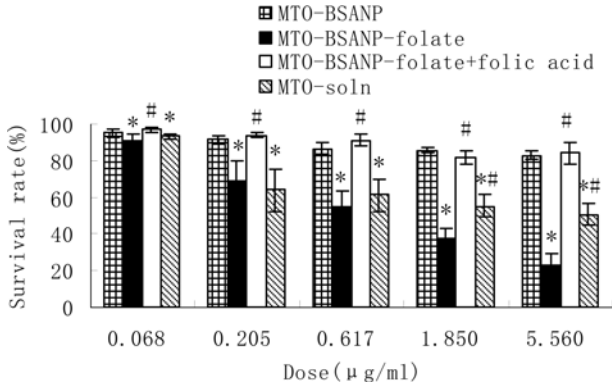

Fig. 4. SKOV3 cells were exposed to MTO solution, MTO-BSANP, MTO-BSANP-folate with or without 1 mmol/L free folic acid for 2 h, then washed and further incubated for 48 h in fresh medium. The survival rate of SKOV3 cells was assayed by ^{3}H-thymidine incorporation. Error bars represent standard deviations (n = 6). *$p < 0.05$, *vs* MTO-BSANP group; $^{\#}p < 0.05$, *vs* MTO-BSANP-folate group.

Table I. Antitumor activity of MTO-BSANP-folate, MTO-BSANP, and MTO solution in SKOV3 tumor bearing mice (n = 5)

Preparations	Tumor weight (g) mean ± S.D.	Inhibition rate (%)
MTO-BSANP-folate	86.36 ± 39.61$^{\#*}$	84.53
MTO-BSANP	179.46 ± 87.41$^{\#}$	67.85
MTO Solution	205.92 ± 53.07$^{\#}$	63.10
Blank	558.12 ± 291.10	-

Note: $^{\#}p < 0.05$, *vs* blank group; *$p < 0.05$, *vs* MTO solution group.

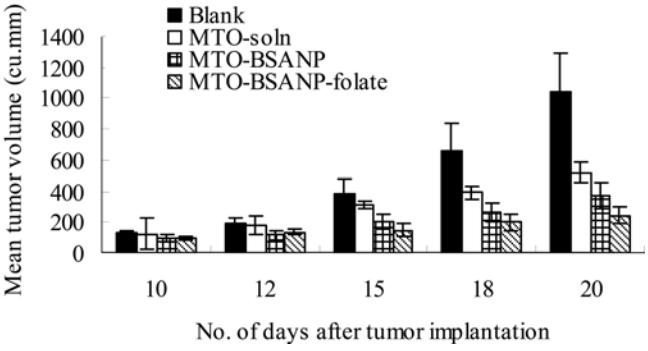

Fig. 5. Changes in tumor volume with different treatments, expressed as mean ± S.D., n=5.

tumor activity. Control mice showed progressive tumor growth over 20 days, with a mean tumor volume on day 10 of 126.9 ± 18.1 mm^3 increasing to 1038.0 ± 250.7 mm^3 10 days later (Fig. 5). The MTO-BSANP group showed a slower growth rate [from 91.7 ± 24.0 mm^3 to 370.9 ± 78.0 mm^3] than the MTO solution group [from 124.3 ± 99.4 mm^3 to 518.8 ± 67.6 mm^3], perhaps because MTO-BSANP could passively accumulate in the tumor tissues via EPR. The group treated with MTO-BSANP-folate showed the smallest increase in tumor volume [from 96.3 ± 17.4 mm^3 to 242.9 ± 56.9 mm^3]. The combined effect of passive accumulation and enhanced intracellular delivery could explain this improved therapeutic efficacy of MTO-BSANP-folate over MTO-BSANP or MTO solution.

CONCLUSIONS

In conclusion, we have demonstrated for the first time that MTO-BSANP-folate enhanced the intracellular uptake of the entrapped MTO by SKOV3 cells to improve antitumor activity by potentiating passive accumulation in tumor tissue and subsequent increased intracellular uptake by folate-mediated endocytosis. These folate-conjugated BSANP may have therapeutic potential as the vector of anticancer drugs.

ACKNOWLEDGEMENTS

This project was supported by the Chongqing Natural Science Foundation (No. CSTC, 2008BB5397) and the Specialized Research Fund for the Doctoral Program of Higher Education of China. (No. 20020610092).

REFERENCES

Atkinson, S. F., Bettinger, T., Seymour, L. W., Behr, J., and Ward, C., Conjugation of folate via gelonin carbohydrate residues retains ribosomal-inactivating properties of the toxin and permits targeting to folate receptor positive cells. *J. Biol. Chem*., 276, 27930-27935 (2001).

Campbell, I. G., Jones, T. A., Foulkes, W. D., and Trowsdale, J., Folate-binding protein is a marker for ovarian cancer. *Cancer Res*., 51, 5329-5338 (1991).

Chan, P., Kurisawa, M., Chung, J. E., and Yang, Y. Y., Synthesis and characterization of chitosan-g-poly(ethylene glycol)-folate as a non-viral carrier for tumor-targeted gene delivery. *Biomaterials*, 28, 540-549 (2007).

Dreis, S., Rothweiler, F., Michaelis, M., Cinatl, J. Jr., Kreuter, J., and Langer, K., Preparation, characterisation and maintenance of drug efficacy of doxorubicin-loaded human serum albumin (HSA) nanoparticles. *Int. J. Pharm*., 341, 207-214 (2007).

Ehninger, G., Schuler, U., Proksch, B., Zeller, K. P., and Blanz, L., Pharmacolinetics and metabolism of mitoxantrone. A review. *Clin. Pharmacokinet*., 18, 365-380 (1990).

Faulds, D., Balfour, J. A., Chrisp, P., and Langtry, H. D., Mitoxantrone. A. review of its pharmacodynamic and pharmacokinetic properties and therapeutic potential in the chemotherapy of cancer. *Drugs*, 41, 400-449 (1991).

Huang, L., Sankar, S., Lin, C., Kontos, C. D., Schroff, A. D.,

Cha, E. H., Feng, S. M., Li, S. F., Yu, Z., Van Etten, R. L., Blanar, M. A., and Peters, K. G., HCPTPA, a protein tyrosine phosphatase that regulates vascular endothelial growth factor receptor-mediated signal transduction and biological activity. *J. Biol. Chem*., 274, 38183-38188 (1999).

Kamen, B. A. and Caston, J. D., Properties of a folate binding protein (FBP) isolated from porcine kidney. *Biochem. Pharmacol*., 35, 2323-2329 (1986).

Langer, K., Balthasar, S., Vogel, V., Dinauer, N., von Briesen, H., and Schubert, D., Optimization of the preparation process for human serum albumin (HSA) nanoparticles. *Int. J. Pharm*., 257, 169-180 (2003).

Lee, R. J. and Low, P. S., Delivery of liposomes into cultured KB cells via folate receptor-mediated endocytosis. *J. Biol. Chem*., 269, 3198-3204 (1994).

Lee, R. J. and Low, P. S., Folate-mediated tumor cell targeting of liposome-entrapped doxorubicin in vitro. *Biochim. Biophys. Acta*, 1233, 134-144 (1995).

Lee, R. J. and Huang, L., Folate-targeted, anionic liposomeentrapped polylysine-condensed DNA for tumor cell-specific gene transfer. *J. Biol. Chem*., 271, 8481-8487 (1996).

Lu, Y. and Low, P. S., Immunotherapy of folate receptor-expressing tumors: review of recent advances and future prospects. *J. Control. Release*, 91, 17-29 (2003).

Lu, B., Xiong, S. B., Yang, H., Yin, X. D., and Zhao, R. B., Mitoxantrone-loaded BSA nanospheres and chitosan nanospheres for local injection against breast cancer and its lymph node metastases I: Formulation and in vitro characterization. *Int. J. Pharm*., 307, 168-174 (2006).

Reszka, R., Beck, P., Fichtner, I., Hentschel, M., Richter, J., and Kreuter, J., Body Distribution of Free, Liposomal and Nanoparticle-Associated Mitoxantrone in B16-Melanoma-Bearing Mice. *J. Pharmacol. Exp. Ther*., 280, 232-237 (1997).

Rubino, O. P., Kowalsky, R., and Swarbrick, J., Albumin microspheres as a drug delivery system: relation among turbidity ratio, degree of cross-linking, and drug release. *Pharm. Res*., 10, 1059-1065 (1993).

Schleyer, E., Kamischke, A., Kaufmann, C. C., Unterhalt, M., and Hiddemann, W., New aspects on the pharmacokinetics of Mitoxantrone and ist two major metabolites. Leukemia, 8, 435-440 (1994).

Shenkenberg, T. D. and Von Hoff, D. D., Mitoxantrone: A new anticancer drug with significant clinical activity. *Ann. Intern. Med*., 105, 67-81 (1986).

Singh, R. and Lillard, J. W. Jr., Nanoparticle-based targeted drug delivery. *Exp. Mol. Pathol*., 86, 215-223 (2009).

Smith, I. E., Mitoxantrone (Novantrone): A review of experimental and early clinical studies. *Cancer Treat. Rev*., 10, 103-115 (1983).

Weber, C., Coester, C., Kreuter, J., and Langer, K., Desolvation process and surface characterisation nanoparticles. *Int. J. Pharm*., 194, 91-102 (2000).

Xiong, X. B., Huang, Y., Lu, W. L., Zhang, X., Zhang, H., Nagai, T., and Zhang, Q., Enhanced intracellular delivery and improved antitumor efficacy of doxorubicin by sterically stabilized liposomes modified with a synthetic RGD mimetic. *J. Control. Release*, 107, 262-275 (2005).

Yang, L., Cui, F., Cun, D., Tao, A., Shi, K., and Lin, W., Preparation, characterization and biodistribution of the lactone form of 10-hydroxycamptothecin (HCPT)-loaded bovine serum albumin (BSA) nanoparticles. *Int. J. Pharm*., 340, 163-172 (2007).

Zhang, Z. R. and Liao, G. T., Studies on mitoxantrone nanospheres for hepatic targeting. In Liao, G.T. (Ed.). Targeted Drug Delivery Systems. Publishing House of Science and Technology, Sichuan, pp. 230-231, (1997).

Zhang, L. K., Hou, S. X., Mao, S. J., Wei, D. P., Song, X. R., and Lu, Y., Uptake of folate-conjugated albumin nanoparticles to the SKOV3 cells. *Int. J. Pharm*., 287, 155-162 (2004).

Zhao, X. B. and Lee, R. J., Tumor-selective targeted delivery of genes and antisense oligodeoxyribonucleotides via the folate receptor. *Adv. Drug Deliv. Rev*., 56, 1193-1204 (2004).